Available online at www.sciencedirect.com

SciVerse ScienceDirect

Procedia Engineering 00 (2015) 000–000

Procedia Engineering

www.elsevier.com/locate/procedia

24th International Meshing Roundtable (IMR24)

A comparison of C^0 and G^1 continuous curved tetrahedral meshes for high-order finite element simulations

Daniel W. Zaide*, Qiukai Lu, Mark S. Shephard

Scientific Computation Research Center, Rensselaer Polytechnic Institute, Troy, NY, 12180-3590, USA

Abstract

This paper examines the effect of curved boundary continuity on finite element simulations. Quartic C^0 continuous and G^1 continuous meshes with curved boundaries are created from CAD geometry. These C^0 continuous and G^1 continuous surface triangles are constructed using Bézier triangles and triangular Gregory patches respectively. Curved tetrahedra are constructed using a shape blending with tetrahedral mapping. The curved meshes are solved on using a high-order finite element method. The effect of surface continuity on solution accuracy is quantified for a simple fluid problem in three dimensions.

Peer-review under responsibility of organizing committee of the 24th International Meshing Roundtable (IMR24).

Keywords: Curved Meshes; Bézier Surfaces; High-order Meshing;

1. Introduction

In order to fully realize the benefits of high-order methods, the curved portions of the geometric domain must be properly represented by the computational mesh. Previous analyses using the relation of approximation theory to the convergence of the error in the energy norm have indicated that numerical solutions will converge as the geometric approximation of the mesh is within one order of that used in the finite element basis [1]. Thus, for proper solution accuracy, the mesh edges and faces representing curved domain geometry must be curved and provide a sufficient order of geometry approximation to prevent the loss of convergence and accuracy due to the geometric approximation [2–5].

Early attempts to accurately represent curved domains for finite element simulations date back to the 1970s when the isoparametric element approach was introduced to solid mechanics applications [6]. With the rapid development of the Computer-Aided Geometric Design (CAGD) technology, researchers started to work on integration of CAD technology for geometrical representation with finite element analysis methods. Schramm and Pilkey [7] used Non-Uniform Rational B-Splines (NURBS), the industry standard for geometric modeling, for geometry to implement transfinite elements and applied it to shape optimization. A number of different techniques have been proposed in recent years to generate curvilinear meshes based on polynomial mappings and optimal nodal placement [8–11].

* Corresponding author.
E-mail address: dan.zaide@gmail.com

Peer-review under responsibility of organizing committee of the 24th International Meshing Roundtable (IMR24).

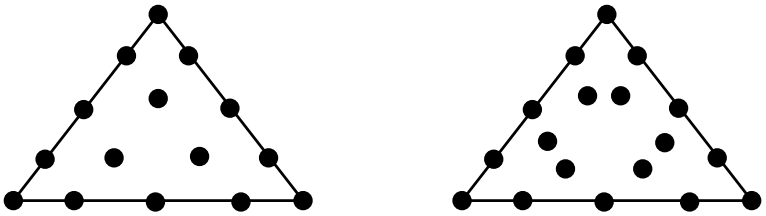

Fig. 1. Control points for fourth-order C^0 (left) and G^1 triangles (right).

More recent work on tetrahedral meshes by Sevilla et al [12] have used NURBS to create a NURBS-enhanced FEM method with NURBS based elements near the CAD model boundary and standard polynomial based finite elements for the interior, demonstrating its improvement on several problems with Maxwell's equations.

Alongside this research, in the past ten years extensive research has been on isogeometric analysis, integrating CAD and finite element methods using the same representation for both the geometry and the finite element solution has been carried out. First introduced by Hughes et al in 2005 [3,13], these approaches have been applied with tensor-product NURBS and Bézier surfaces and demonstrated on a wide range of physical problems from structural mechanics to fluid-structure interaction problems [14]. These methods also easily support higher order interelement continuity, allowing for higher than C^0 continuous surfaces. The increase in continuity has led to $k-$refinement, and demonstrated increased accuracy on structural mechanics problems with quadrilateral and hexahedral meshes [15]. On triangular meshes, these ideas are only beginning to be explored. In 2012, Speleers et al [16] used quadratic Powell-Sabin splines (NURPS) for advection-diffusion problems on triangular domains and then in 2014, Jaxon and Qian [17] used rational triangular Bézier splines to represent their two dimensional geometries. With the challenges of isogeometric analysis on triangles, we focus on an alternative approach for tetrahedral meshes to determine if some of their benefits can also be obtained, specifically the effect of surface continuity.

Outside of isogeometric analysis, it has been previously determined that certain types of physical applications, such as electromagnetic scattering and compressible flow applications, are sensitive to both the accuracy and smoothness of the computational mesh that approximates the curved domain boundaries [4,12]. On most curved tetrahedral meshes, representations of triangular boundary faces focus on treating each face as an individual curved element, resulting in C^0 continuous surface patches. By considering neighboring boundary faces, continuity of surface normals can be achieved, described as G^1 continuous. G^1 geometrically continuous surfaces have been around since 1974 when Gregory [18] introduced the idea for quadrilateral surfaces. Walton and Meek [19] later developed the triangular version used in this work, and it has since been extended and applied [20,21] to higher orders for computer graphics applications. Geometrically continuous surfaces have been used in meshing applications as well, with Owen et al [22] using them to create a smooth geometry representation from a faceted input in the common geometry module and Frey [23] using them to support curved surface meshes and provided enhanced geometric information in the absence of underlying CAD.

In this paper, we introduce a preliminary study of the effects of surface triangle continuity on finite element simulations, comparing a quartic C^0 continuous Bézier surface with a quartic G^1 continuous surface representation. Our meshing software [24] is integrated into Nektar++ [25], a high-order finite element solver. A simple pipe flow in three dimensions is studied and the accuracy is quantified. This work will provide insight into future directions for more in-depth studies in node placement and curved surface representation as we continue to improve high-order meshes.

2. Curved Meshes

We compare the effect of surface patch continuity using quartic, fourth-order C^0 and G^1 triangles. Fourth-order triangles are used for the comparison as it is the minimum order needed for G^1 continuity. We obtain C^0 continuous surface triangles using Bézier triangles, defined by the 15 control points [26] in Figure 1. To determine the control point locations on the CAD geometry, we use interpolating Bézier triangles, first determining interpolation points using points in the surface parametrization from Chen and Babuška [27] and then solving for the control points. To construct G^1 triangles, we follow the work of Walton and Meek [19]. Their approach results in a G^1 continuous

quartic surface, represented by 18 control points, three more than required for a similar Bézier triangle, as shown in Figure 1. Geometric continuity is obtained by constraining tangential derivatives across boundary edges. In order to obtain the required G^1 continuity, the cross-boundary tangent fields associated with the three mesh edges have to be satisfied simultaneously, thus requiring more degrees of freedom than a quartic triangular Bézier patch. As a result, an additional three control points. Unlike the Bézier triangle, the edges of the G^1 triangle are determined using the the point locations and normals at each vertex to determine the cubic control points. The internal points, are then determined such that the any two adjoining triangles have a common tangent plane. We refer the reader to [19] for more details.

In our curved mesh, we use the blending approach of Dey et al [1]. In the conventional isoparametric approach with C^0 meshes, the volumetric mapping between a standard parametric space and the physical space is constructed based on the same polynomial basis functions used for the finite element space. However, the basis functions used to represent the rational G^1 curved mesh are generally not the same as the finite element shape functions used for analysis. Therefore, a more general approach is adopted to construct the volumetric mapping in order to account for the G^1 surface geometry. The shapes of lower dimensional mesh entities bounding the element volume are multiplied with quadratic blending functions, and the contributions are summed together to get the complete volume mapping.

The equation for the mapping is given in Eq (1) as

$$\begin{aligned} x_i(\boldsymbol{\xi}) = {} & (1-\xi_1)^{k+1} F_1(\xi'_{F_1}) + (1-\xi_2)^{k+1} F_2(\xi') + (1-\xi_3)^{k+1} F_3(\xi') + (1-\xi_4)^{k+1} F_4(\xi') - (1-\xi_1-\xi_2)^{k+1} E_1(\xi') \\ & -(1-\xi_1-\xi_3)^{k+1} E_2(\xi') - (1-\xi_1-\xi_4)^{k+1} E_3(\xi') - (1-\xi_2-\xi_3)^{k+1} E_4(\xi') - (1-\xi_2-\xi_4)^{k+1} E_5(\xi') \\ & -(1-\xi_3-\xi_4)^{k+1} E_6(\xi') + \xi_1^{k+1} V_1 + \xi_2^{k+1} V_2 + \xi_3^{k+1} V_3 + \xi_4^{k+1} V_4 \end{aligned} \tag{1}$$

where $\boldsymbol{\xi} = (\xi_1, \xi_2, \xi_3, \xi_4)$ are barycentric coordinates and F_i, E_i, and V_i are the positions corresponding to the bounding faces, edges, and vertices. ξ' defines a normalized parametric coordinate on the edge or face, for example on edge E_1, $\xi_1 = \xi_2 = 0$, and $\xi' = (\xi'_1, \xi'_2) = \left(\frac{\xi_3}{\xi_3+\xi_4}, \frac{\xi_4}{\xi_3+\xi_4}\right)$. The blending approach is independent of the chosen face and edge parametrization and thus can be used with both types of curved faces. The choice of k in the blending functions determines the smoothness of the blending functions, and it can be shown that this particular volumetric mapping is C^k continuous. In this work, we use $k = 1$ for a C^1 continuous mapping, though in the future this can be investigated in more detail.

3. Implementation

Our curved meshes are implemented into Nektar++ [25], a high-order finite element code for solving partial differential equations. Nektar++ has a wide range of physics implemented, and is a well validated solver to test the effects of curved meshes. Nektar++ has already been used with curved meshes [8,28] and supports curved meshes defined by standard interpolation functions, describing curved entities by sets of interpolating points.

To integrate our meshing librares within Nektar++, only several small changes are required. First, the XML based input format is adjusted to contain information about our mesh and CAD model files, rather than contain the entire mesh and its connectivity. After the input file is read, our curved mesh and CAD model are loaded, and we overload the edge, triangular face, and tetrahedron geometry classes to store our mesh entities and query them for geometric information. The existing curved framework is used with support for deformed elements. This occurs in two places: first, the coordinates and second, the spatial derivatives. Both are set to call the our API for any edge, face, or tetrahedral element rather than the original geometric functions.

4. Numerical Results - Hagen-Poiseuille Flow

To test the effect of surface continuity, we solve a Hagen-Poiseuille flow problem for the incompresible Navier-Stokes. Hagen-Poiseuille flow describes a fully developed, laminar viscous flow through a circular pipe. In this example, the geometry is a cylinder with unit radius and length 10 in the z-direction. The exact solutions for the

z-velocity and pressure are

$$u_z(\mathbf{x}) = -\frac{1}{4\nu}\left(\frac{\mathrm{d}p}{\mathrm{d}z}\right)(R^2 - r^2), \qquad p(\mathbf{x}) = 1 - \frac{z}{10}, \qquad r^2 = x^2 + y^2 \tag{2}$$

with the radial velocities, $u_x = u_y = 0$. The kinematic viscosity is chosen to be 0.025 such that the velocity profile is $u_z = 1 - r^2$. The inlet to the pipe consists of the velocity flow profile with the outlet specified by standard Neumann boundary conditions on velocity, and a pressure of zero. We solve the problem with a fifth order and sixth order method on mesh consisting of 941 tetrahedra. Geometric accuracy is measured using the maximum interpolation error on the boundary, a representation of the Hausdorff distance. To measure solution accuracy, the L_2, and L_∞ norms of the error, along with the L_2 norm of first derivative error, defined as

$$\begin{aligned} L_2(u^{h,p}) &= \left(\int_{\Omega_M} (u^{h,p} - u_{exact})^2 \, \mathrm{d}\Omega_M\right)^{1/2}, \qquad L_\infty(u^{h,p}) = \max_{\Omega_M} \left|u^{h,p} - u_{exact}\right| \\ L_2(\nabla u^{h,p}) &= \left(\int_{\Omega_M} \nabla(u^{h,p} - u_{exact}) \cdot \nabla(u^{h,p} - u_{exact}) \, \mathrm{d}\Omega_M\right)^{1/2} \end{aligned} \tag{3}$$

are used. A summary of results is in Table 1.

Comparing the interpolation error, the G^1 surface is two orders of magnitude higher than that of the C^0 surface. This is expected, as the control points are used to ensure G^1 continuity rather than directly interpolate the surface. Comparing the errors in x-velocity, the C^0 method outperforms the G^1 method (and does so for both other velocities). Examining the error in pressure, for both the fifth and sixth order method, the L_2 norm is smaller for the C^0 meshes, however both the L_∞ norm of solution error and L_2 norm of the derivative error are smaller, suggesting G^1 continuity may improve the accuracy of derivatives and engineering quantities such as shear stresses. For the G^1 continuous surfaces, the effect of increased surface continuity appears to be mitigated by the larger interpolation error, resulting in a minimal increase in solution accuracy as we go from fifth to sixth order. This is consistent with previous results using Nektar++ [29].

Table 1. Summary of Results for Hagen-Poiseuille Flow, Error in x-velocity and pressure.

	p	Interp. Error	$L_2(u^{h,p})$	$L_\infty(u^{h,p})$	$L_2(\nabla u^{h,p})$	$L_2(p^{h,p})$	$L_\infty(p^{h,p})$	$L_2(\nabla p^{h,p})$
C^0	5	1.19×10^{-5}	2.14×10^{-4}	8.57×10^{-4}	6.34×10^{-3}	1.71×10^{-3}	2.40×10^{-2}	5.50×10^{-2}
G^1	5	6.32×10^{-3}	1.22×10^{-3}	1.67×10^{-3}	1.36×10^{-2}	4.51×10^{-3}	5.25×10^{-3}	2.75×10^{-2}
C^0	6	1.19×10^{-5}	8.12×10^{-5}	3.10×10^{-4}	2.43×10^{-3}	4.40×10^{-4}	6.85×10^{-3}	2.12×10^{-2}
G^1	6	6.32×10^{-3}	1.21×10^{-3}	1.65×10^{-3}	1.30×10^{-2}	4.47×10^{-3}	4.61×10^{-3}	1.77×10^{-2}

These results do not demonstrate an obvious advantage to G^1 continuity of the mesh. The potential benefits of surface continuity are outweighed by the additional effort in their formulation. While Bézier triangles can be naturally extended to arbitrary order, obtaining fifth-order G^1 triangles is non-trivial [20,21], and sixth order and higher formulations do not currently exist. Given the control points of a higher-order surface triangle, using the control points to reduce interpolation error or improve other aspects of mesh quality instead of increasing the level of interelement appears to be the appropriate option. In the absence of CAD geometry, there may be more interest in G^1 continuity, however if the CAD geometry is available, it is likely not advantageous.

5. Conclusions and Future Work

In this paper, the effects of C^0 continuity compared to G^1 surface triangle continuity for curved tetrahedral meshes are examined. For a simple flow problem, meshes with fourth order G^1 continuous surface patches do not significantly improve solution accuracy compared to similar fourth order C^0 continuous patches. The increased interpolation error of G^1 triangles appears to outweight the potential benefits. As geometric continuity is far from the only factor at play, further work is needed to study relevant metrics such as the scaled Jacobian for optimal control point locations to improve solution accuracy.

The next step is to determine whether G^1 is worth pursuing further by applying it to more problems and examining its effect on forces, stresses, and other engineering quantities. If there is shown to be a significant advantage, fifth order and higher G^1 triangles will be investigated. This will allow for investigation of their effects on highly anisotropic problems, such as boundary layer problems.

Additional developments of importance for high order curved meshes simulations include improvements to the algorithms for adaptive mesh refinement, coarsening, swapping in combination with mesh entity reshaping opportunities afforded when using high order mesh geometry.

References

[1] S. Dey, M. S. Shephard, J. E. Flaherty, Geometry representation issues associated with p-version finite element computations, Computer Methods in Applied Mechanics and Engineering 150 (1997) 39 – 55. Symposium on Advances in Computational Mechanics.

[2] X. Luo, M. S. Shephard, J.-F. Remacle, R. M. O'Bara, M. W. Beall, B. Szabo, R. Actis, P-version mesh generation issues, in: 11th International Meshing Roundtable, Ithaca, NY., 2002, pp. 343–354.

[3] T. J. R. Hughes, J. Cottrell, Y. Bazilevs, Isogeometric analysis: CAD, finite elements, NURBS, exact geometry and mesh refinement., Computer Methods in Applied Mechanics and Engineering. 194 (2005) 4135–4195.

[4] L. Demkowicz, P. Gatto, W. Qiu, A. Joplin, G1-interpolation and geometry reconstruction for higher order finite elements, Computer Methods in Applied Mechanics and Engineering 198 (2009) 1198–1212.

[5] Q. Lu, M. S. Shephard, S. Tendulkar, M. W. Beall, Parallel mesh adaptation for high-order finite element methods with curved element geometry, Engineering with Computers 30 (2014) 271–286.

[6] O. C. Zienkiewicz, The Finite Element Method in Engineering Science, second ed. ed., London: McGraw-Hill, 1971.

[7] U. Schramm, W. Pilkey, The coupling of geometric descriptions and finite elements using NURBs – a study in shape optimization, Finite Elements in Analysis and Design. 15 (1993) 11–34.

[8] S. J. Sherwin, J. Peiro, Mesh generation in curvilinear domains using high-order elements, International Journal for Numerical Methods in Engineering 53 (2002) 207–223.

[9] P.-O. Persson, J. Peraire, Curved mesh generation and mesh refinement using lagrangian solid mechanics, in: 47th AIAA Aerospace Sciences Meeting and Exhibit., 2009.

[10] A. Johnen, J.-F. Remacle, C. Geuzaine, Geometrical validity of curvilinear finite elements, in: 20th International Meshing Roundtable, 2011.

[11] A. Gargallo-Peiró, X. Roca, J. Sarrate, A surface mesh smoothing and untangling method independent of the cad parameterization, Computational Mechanics 53 (2014) 587–609.

[12] R. Sevilla, S. Fernández-Méndez, A. Huerta, 3d nurbs-enhanced finite element method (nefem), International Journal for Numerical Methods in Engineering 88 (2011) 103–125.

[13] J. A. Cottrell, T. J. Hughes, Y. Bazilevs, Isogeometric analysis: toward integration of CAD and FEA, John Wiley & Sons, 2009.

[14] Y. Bazilevs, V. M. Calo, J. A. Cottrell, J. A. Evans, T. Hughes, S. Lipton, M. Scott, T. Sederberg, Isogeometric analysis using t-splines, Computer Methods in Applied Mechanics and Engineering 199 (2010) 229–263.

[15] J. Cottrell, T. Hughes, A. Reali, Studies of refinement and continuity in isogeometric structural analysis, Computer methods in applied mechanics and engineering 196 (2007) 4160–4183.

[16] H. Speleers, C. Manni, F. Pelosi, M. L. Sampoli, Isogeometric analysis with powell–sabin splines for advection–diffusion–reaction problems, Computer methods in applied mechanics and engineering 221 (2012) 132–148.

[17] N. Jaxon, X. Qian, Isogeometric analysis on triangulations, Computer-Aided Design 46 (2014) 45–57.

[18] J. A. Gregory, Smooth interpolation without twist constraints, Brunel University Mathematics Technical Papers collection; (1974).

[19] D. J. Walton, D. S. Meek, A triangular g 1 patch from boundary curves, Computer-Aided Design 28 (1996) 113–123.

[20] W.-h. Tong, T.-w. Kim, High-order approximation of implicit surfaces by G^1 triangular spline surfaces, Computer-Aided Design 41 (2009) 441–455.

[21] G. Farin, D. Hansford, Agnostic g 1 gregory surfaces, Graphical Models 74 (2012) 346–350.

[22] S. J. Owen, D. R. White, T. J. Tautges, Facet-based surfaces for 3d mesh generation. (2002) 297–311.

[23] P. J. Frey, About surface remeshing (2000).

[24] D. A. Ibanez, E. S. Seol, C. W. Smith, M. S. Shephard, Pumi: Parallel unstructured mesh infrastructure, ACM Transactions on Mathematical Software, submitted (2014).

[25] C. Cantwell, D. Moxey, A. Comerford, A. Bolis, G. Rocco, G. Mengaldo, D. De Grazia, S. Yakovlev, J.-E. Lombard, D. Ekelschot, et al., Nektar++: An open-source spectral/hp element framework, Computer Physics Communications 192 (2015) 205–219.

[26] G. Farin, Triangular bernstein-bézier patches, Computer Aided Geometric Design 3 (1986) 83–127.

[27] Q. Chen, I. Babuška, Approximate optimal points for polynomial interpolation of real functions in an interval and in a triangle, Computer Methods in Applied Mechanics and Engineering 128 (1995) 405–417.

[28] D. Moxey, D. Ekelschot, Ü. Keskin, S. Sherwin, J. Peiró, A thermo-elastic analogy for high-order curvilinear meshing with control of mesh validity and quality, 23rd International Meshing Roundtable 82 (2014) 127–135.

[29] C. D. Cantwell, S. Yakovlev, R. M. Kirby, N. S. Peters, S. J. Sherwin, High-order spectral/hp element discretisation for reaction–diffusion problems on surfaces: Application to cardiac electrophysiology, Journal of computational physics 257 (2014) 813–829.